

Shape Optimization of Composite Structure under Uncertainty

J. Auzins, A. Janushevskis, A. Melnikovs, J. Janushevskis

Abstract—The developed methods and software tool for robust optimization have been tested on the two bar truss problem and applied to the shape optimization of the new composite pallet structure. Sensitivity analyses for probabilistic performances are given. Deterministic structural shape optimization problem of pallet is solved in the first stage. Next the same problem is considered as non-deterministic taking into account possible uncertainties of supporting conditions. The obtained results from deterministic and non-deterministic optimization are compared and appropriate solution for design of pallet is proposed.

Keywords—composite structures, metamodeling, robust optimization, shape optimization.

I. INTRODUCTION

POWERFUL methods for shape and topology optimization of mechanical engineering objects such as ground structure [1], homogenization [2] and solid isotropic material with penalization [3] are broadly used for industry problem solving. Popular new approaches for shape optimization are morphing, implicit parameterization and CAD-based direct parameterization [4], [5], [6]. Nevertheless real life problems are almost always non-deterministic. Uncertainties appear for example due to material, load and geometry fluctuations: manufacturing tolerances, model errors, changing environments and noisy measurements. Robust optimization approaches [7], [8], [9], and [10] seek to limit the effects in quality of the solutions due to uncertainties.

In recent years the CAD-based direct parameterization approaches [11] have become highly effective and popular due to rapid development of the integrated CAD/CAE software systems and advanced metamodeling techniques [12], [13], [14], and [15]. NURBS utilization for the freeform curves representation of CAD models can give even more benefits for

This work has been supported by the European Social Fund within the Project No. 2013/0025/1DP/1.1.1.2.0/13/APIA/VIAA/019 “New “Smart” Nanocomposite Materials for Roads, Bridges, Buildings and Transport Vehicle”.

J. Auzins is Corresponding Member of the Latvian Academy of Science and with the Institute of Mechanics, Riga Technical University, Riga, Latvia (phone: +371 67089396; e-mail: auzinsj@latnet.lv).

A. Janushevskis is Head of Machine and Mechanism Dynamics Research Laboratory with the Institute of Mechanics, Riga Technical University, Riga, Latvia (e-mail: janush@latnet.lv).

A. Melnikovs is with the Institute of Mechanics, Riga Technical University, Riga, Latvia (e-mail: anatolijs.melnikovs@inbox.lv).

J. Janusevskis is with the Institute of Mechanics, Riga Technical University, Riga, Latvia (e-mail: janisj@latnet.lv).

those techniques. Also references to the kriging based optimization methods [16] and [17] are commonly given to solve deterministic optimization problems. For non-deterministic optimization problems, such as composite structures that account for uncertainties, the optimization is usually based on double loop approaches where the uncertainty propagation is recursively performed inside the optimization iterations. Often the uncertainty estimation for the given point is based on a meta-model, thus allowing reduction of computational time but introducing additional bias in the estimates. In the previous work [18] a single loop kriging based method for minimizing the mean of an objective function is proposed: simulation points are calculated in order to simultaneously propagate uncertainties, i.e., estimate the mean objective function, and optimize this mean.

II. KEDRO SOFTWARE

KEDRO (previous name EDAOpt) was originally developed as a collection of non-gradient-based optimization software. KEDRO now includes methods and tools for statistical data sampling, approximation and metamodeling methods, and metamodel-based multiobjective optimization.

KEDRO and CAE simulation code (mainly FE, CFD and multibody dynamics software) remain entirely independent, with data being transferred between KEDRO and the simulation code through writing and reading text files. KEDRO does not require access to the source code of the user's simulation software.

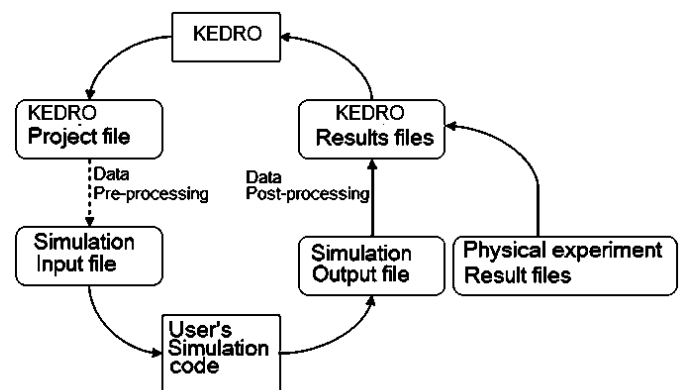


Fig. 1 Information exchange between KEDRO, user-supplied simulation code and experimental equipment

Fig. 1 shows the information exchange between KEDRO,

simulation software and physical experiment equipment.

Fig. 2 shows a typical flowchart of metamodeling-based optimization. Different optimization software packages may use different components for each stage, but the principle remains the same.

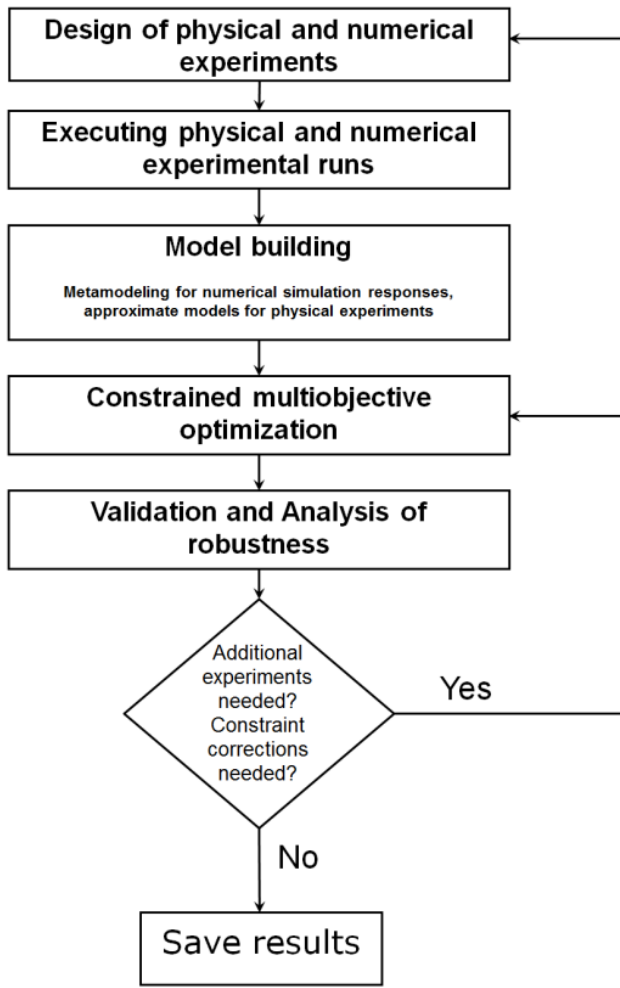


Fig. 2 The flowchart of metamodel-based optimization

Fig. 3 shows the main capabilities of KEDRO software for experimental design, analysis and multiobjective robust optimization using physical and numerical experiments.

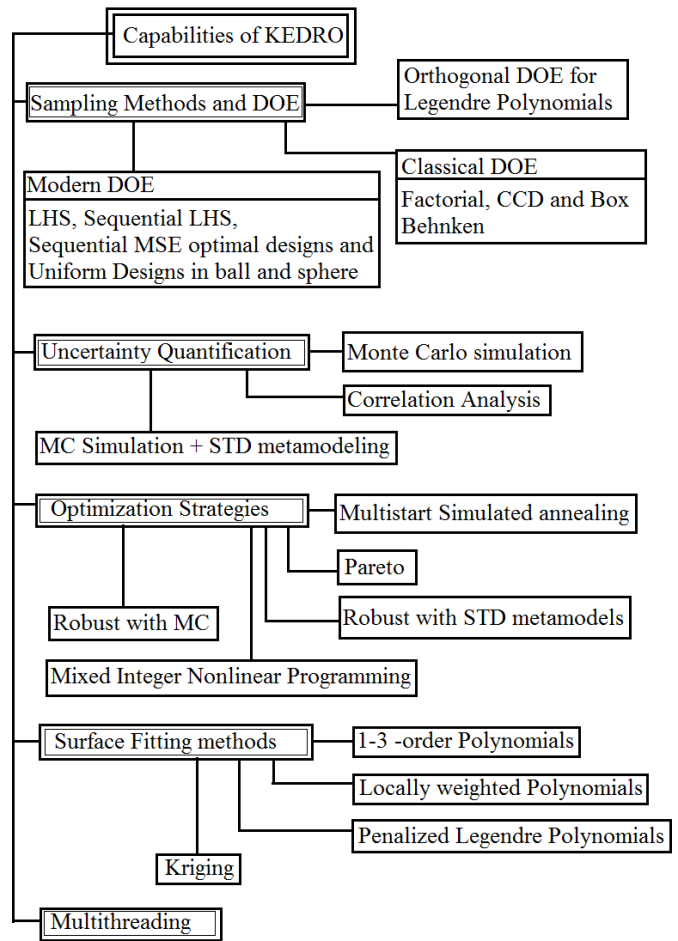


Fig. 3 Capabilities of the KEDRO software

III. CASE STUDY 1: TWO BAR TRUSS

Here we demonstrate the use of KEDRO for the two-bar truss optimization, which is a popular testing example for metamodeling, constrained optimization and robust optimization [19].

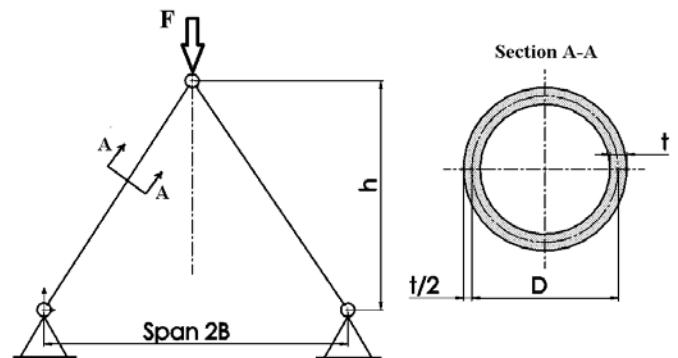


Fig. 4 Two-bar truss

The two-bar test case aims at designing a structure made of two cylindrical bars joined together at the top as shown in Fig. 4. A downwards force F is applied to the top of the structure.

The design variables are the bar diameter D and structure height h . The objective is to minimize the total volume V . Buckling and strength failures give the formulation constraints:

$$\min_{D, h} V \text{ such that } \sigma \leq \sigma_{\max} \text{ and } \sigma \leq \sigma_{\text{crit}} \quad (1)$$

where σ is the stress on the bar, σ_{\max} is the yield strength, and σ_{crit} is the maximum buckling load. The two-bar problem is simple enough to have analytical expressions for the objective function and constraints:

$$2\pi D t \sqrt{B^2 + h^2}, \quad \sigma = \frac{F \sqrt{B^2 + h^2}}{2\pi D h}, \quad \sigma_{\text{crit}} = \frac{\pi^2 E (D^2 + t^2)}{8(B^2 + h^2)} \quad (2)$$

For the robust optimization we have two design variables D and h , and additional four parameters – constants with fluctuations (unmapped analysis variables, see [20]). All parameter nominal values and their standard deviations are given in Table I.

Table I. Two-bar truss parameters. The fluctuations around the nominal values are Gaussian and all parameters are independent of each other

Parameter	Nominal value	Std. Dev.
D bar diameter (mm)	20-80	1
t bar wall thickness (mm)	2.5	0.1
h structure height (mm)	278-936	3
B half structure width (mm)	750	5
E Young's modulus (N/mm ²)	210000	21000
F applied force (N)	150000	15000
s_{\max} Yield strength (N/mm ²)	400	-----

The solution of the deterministic problem is $D = 37.876$ mm, $h = 608.89$ mm, in which case $V = 0.5747631$ dm³, $\sigma = 399.99995$ N/mm², $\sigma_{\text{crit}} = 400.00019$ N/mm².

To show the possibilities of metamodeling, we will use numerical experiments by calculating the response functions V , σ , σ_{crit} according to the design of experiments. We will use 6 input factors for metamodels. Table II shows the notation and limits of variation for all input factors

Table II Two-bar truss parameters. The fluctuations around the nominal values are Gaussian and all parameters are independent of each other

Factor = Parameter	Limits
$x_1 = D$	20-80
$x_2 = t$	2.4-2.6
$x_3 = h$	278-936
$x_4 = B$	745-755
$x_5 = E$	190000-230000
$x_6 = F$	120000-150000

111-point 6-factor MSE optimized design of experiments was used. The limits for “noisy constants” x_2, x_4, x_5, x_6 were set \pm one standard deviation from nominal value.

The responses are y_1 – stress σ , y_2 – buckling stress σ_{crit} and y_3 – volume V . The accuracy of approximation for tests with known response functions f_{test} was measured with the relative average prediction error σ_{test} in additional confirmation points not used in model building

$$\sigma_{\text{test}} = 100\% \frac{\sqrt{\frac{1}{N} \sum_{i=1}^N (f_{\text{test}}(z_i) - \hat{f}_{\text{test}}(z_i))^2}}{\sqrt{\frac{1}{N} \sum_{i=1}^N (f_{\text{test}}(z_i) - \bar{f}_{\text{test}})^2}} = 100\% \sqrt{\frac{\text{MeanSquareError}}{\text{Variance}}} \quad (3)$$

where z_i – confirmation points ($i=1, \dots, N$), $\hat{f}_{\text{test}}(w_i)$ – approximated value of test function, \bar{f}_{test} – average value of test function in confirmation points. 100000 uniformly randomly selected confirmation points (Latin hypercube sample) were used in the region of interest.

The kriging approximation was used for all three responses. The greatest approximation relative error was f or y_1 – 1.53%. Fig. 5 shows the relative cross-validation 1.95%, in most cases the cross-validation error is pessimistic – the actual error is less than the cross-validation prediction. 1.53% is a good result; if the error would be measured relative to the full range of the change of the stress response (1087N/mm²), the relative error would be 0.28%.

TestSigma=1.52915901975475%

Functions Yt	Strength	CrStrength	Volume
Method	Kriging		Kriging
Sigma Cross	3.933738	1.758704	287.692699
Sigma Cross%	1.952612%	0.314628%	0.101197%
Sigma	0.000179	0.000002	0.022784
Sigma%	0.000089	0.000000	0.000008
Sigma0	0.000185	0.000003	0.023538
Sigma0%	0.000092	0.000000	0.000008
MeanExpValue	384.541103	801.853137	766800.103027
StDev of Exp	201.460314	558.979362	284291.025622
Exp. Range	1087.954072	2492.878252	1224913.739257
MaxError	-0.000694	-0.000009	0.065113
Bad Point No.	82	59	84
Max Rel Error	0.00%	0.00%	0.00%
BadRelPointNo.	82	61	84
No. of Actual Exp	111	111	111

Fig. 5 Kriging approximation results

The solution of the deterministic problem is $D = 37.876$ mm, $h = 608.89$ mm, in which case $V = 0.5747631$ dm³, $\sigma = 399.99995$ N/mm², $\sigma_{\text{crit}} = 400.00019$ N/mm².

Table III shows the deterministic and robust optimization results for exact mathematical models and kriging metamodels. The optimization results obtained by the 111-run 6-factor experimental design are relatively close to the result obtained

by using the exact mathematical model. It must be noted that the difference between the metamodel and the exact model is less than the standard deviation system parameters. The optimization method used was the reliability type optimization [19] and [20] and requires 95% probability of satisfaction both constraints (1).

Table III The results of two-bar truss optimization. Robust optimization with 95% confidence probability

	Deterministic exact	Robust exact 95%	Deterministic metamodels	Robust metamodels 95%
D	37.88	46.61	37.95	45.53
h	608.89	711.65	611.23	747
V	0.574763	0.75713	0.576746	0.757050
Worst case V	0.631675	0.82869	0.622671	0.815109
$\bar{\sigma}$	399.9999	297.65	399.99	481.14
5th and 95th percentile σ	235-567	194-400	-----	198-400
$\bar{\sigma}_{crit}$	400.00128	528	400	481
5th and 95th percentile σ_{crit}	307-493	409-645	-----	398-568

IV. CASE STUDY 2: PALLET SHAPE OPTIMIZATION

Nowadays wood pallets are often replaced by composite pallets due to obvious benefits - superior strength and weight ratio, nestable design concept, increased service life, better corrosion and impact resistance, and many others depending on area of application. The proposed new design of composite pallet (with dimensions 1200x800x160mm) (Fig. 6) could be a solution for modern automated distribution systems if its design is able to carry loads up to 19620 N during operation conditions with the factor of safety (FOS) of at least 2. For this reason fiber-reinforced polymer (FRP) [21] compression molding process [22] must be used for pallet manufacturing and also appropriate shapes of strengthening ribs 1-3 (Fig. 6) must be found for maximal performance of the structure.

At the beginning of the previously developed optimization loop [23] and [18], we need to minimize the number of required parameters to accurately specify shapes of strengthening ribs of the pallet. We want to consider only smooth shapes for stiffness ribs that at same time are effective from the aspect of structural integrity. Therefore, due to the symmetry of the pallet the shape effective parameterization with 4 parameters (X1, X2, X3 and X4) is proposed, as shown in Fig. 7. The shape of each stiffness rib is controlled by control points of a non-uniform rational basis spline (NURBS) polygon. The shape is controlled using a small number of parameters that is important for successful optimization, especially for the non-deterministic case.

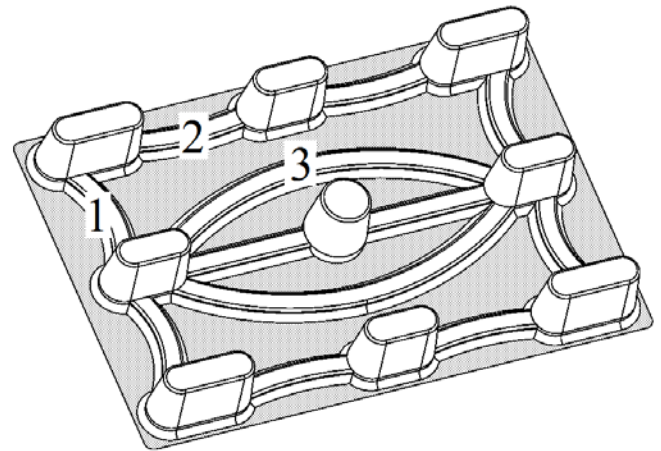


Fig. 6 3D model of loaded pallet and its stiffness ribs 1-3

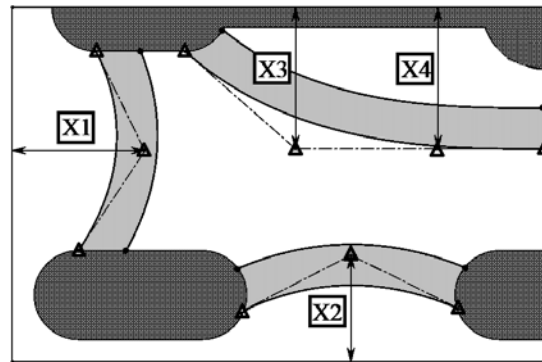


Fig. 7 NURBS parameterization of pallets stiffness ribs in 1/4 pallet layout

The composite material of the pallet consists of two plies of FRP (Table IV), each has 3 mm thickness. The fibers of the second ply are orientated perpendicular to the fibers of the first ply (Fig. 8) in XY plane that provides high strength in both X and Y directions. The strength of the pallet is defined with FOS using the Tsai-Wu criterion [24] which is best applied to orthotropic FRP that has unequal strength in tension and compression. The shell finite elements model of the composite pallet is considered and solved as a multi-ply structure (Fig. 9), taking into account the symmetry of the pallet structure.

Table IV Mechanical properties of FRP

Elastic Modulus	EX = 40000 MPa; EY = 10000 MPa; EZ = 10000 MPa
Poisson's Ratio	NUXY = 0.26; NUYZ = 0.25; NUXZ = 0.26
Shear Modulus	XY = 4500 MPa; YZ = 4000 MPa; XZ = 4500 MPa
Mass Density	$\rho = 1900 \text{ kg/m}^3$
Tensile Strength	SIGXT = 1060 MPa
Compressive Strength	SIGXC = 600 MPa
Shear strength	SIGXY = 70 MPa

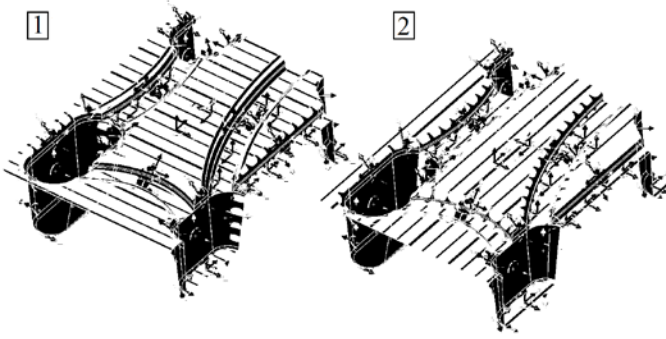


Fig. 8 Definition of fibers directions in 2 plies for 1/4 of 3D model

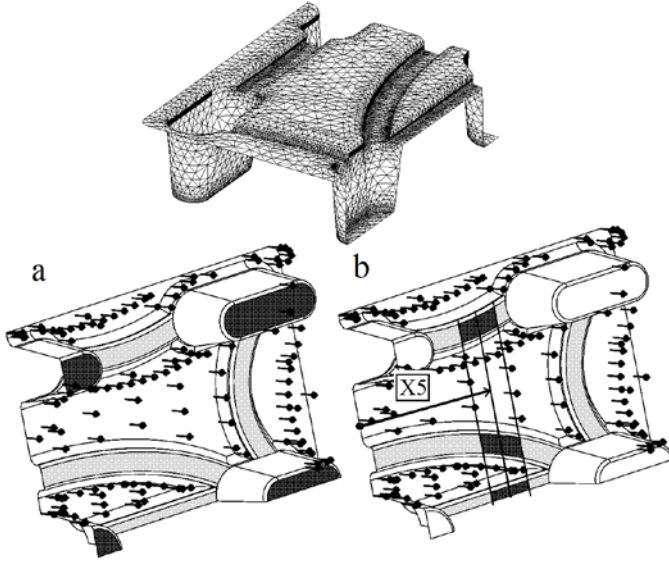


Fig. 9 The shell FE model of 1/4 pallet, and operation cases (a) & (b): arrows – load direction, areas colored black - supporting areas

Two main operation cases of the loaded pallet are simulated: (a) the pallet stays on the rigid basis and (b) the pallet is transported on forks (Fig. 9). In both operation cases the load is assumed to be deterministic and uniformly distributed and applied normally downward to the top surface of the pallet. The case (b) cannot be solved solely as deterministic problem due to uncertainties of supporting conditions (the distance between forks of the lifting equipment is variable). Therefore in the case (b) the problem of the rib shape optimization must take into consideration the random uncertainty in the pallet supports. It is assumed to be symmetric but non-deterministic: supporting areas have constant width but different support placements – X5 on the stiffness ribs as shown in Figs. 9b & 10(I-II).

The results of finite elements analysis show obvious importance of the rib shapes for pallet structure stiffness and strength properties. Also a known fact is confirmed: pallet case (b) causes higher deflection and lower FOS. Therefore, only case (b) is considered during optimization.

Next the deterministic shape optimization problem is defined:

$$\min_{X_n} \delta \quad \text{such that } FOS \geq 2 \text{ and } m \leq 4.688 \quad (4)$$

where X_n = factors X1-X5; δ = pallet maximal deflection; and m = pallet mass. In the first step X5 is assumed taking 2 extreme values: the results are shown in Fig. 10(I-II) and in Table V for each case. By moving supporting conditions to the side of the pallet (increasing X5), the maximal deflection of the pallets tends to relocate from the side of pallet to the center part (Fig. 11) and at same time the level of deflections decreases.

Table V The results of pallet shape optimization

	Range, mm	Optimization cases (see Fig. 10)		
		I	II	III
X1	95-220	182.6448	192.5575	219.827
X2	25-220	79.7038	62.8432	114.209
X3	135-195	135		
X4	160-195	160		
X5	200-270	200 (fixed)	270 (fixed)	160-270
FOS	metamodels	2	2.5	4.72*
	actual	2.2	2.53	
δ , mm	metamodels	3.6869	1.7313	4.719*
	actual	3.6806	1.7213	
m, kg		4.688		4.695*

* 96th percentile

In the next step robust optimization is performed. The uncertainty in X5 is assumed uniform and is propagated using MC simulations on kriging metamodels. The constant number of MC simulations 10E4 is used which is further increased to 10E6 when higher MC accuracy is needed. The 96th percentile is used for criterion and constraint satisfaction. Obtained stiffness ribs shapes and indices are shown on Fig. 10(III) and in Table 5.

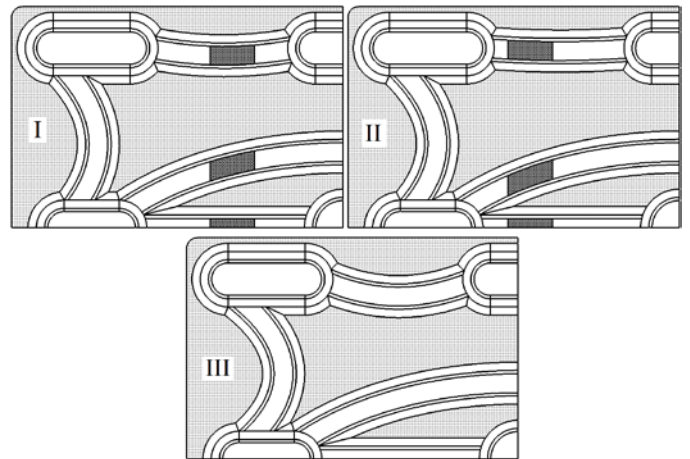


Fig. 10 The results of stiffness ribs shape optimization in 1/4 3D model of pallet for case (b): deterministic optimization for I) X5=200 and II) X5=270; III) robust optimization (the fluctuations around the nominal values are uniform)

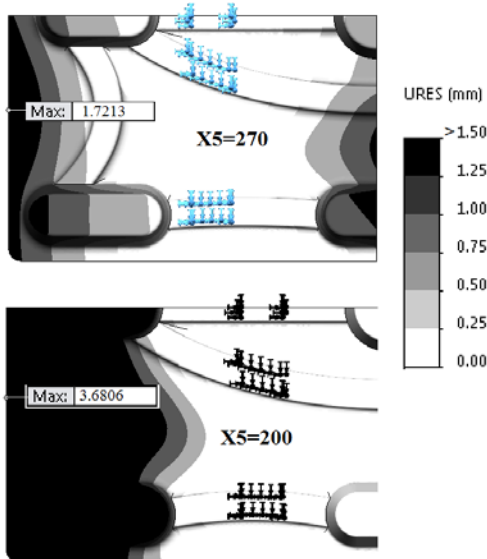


Fig. 11 The maximal deflection of the pallet for case (b): deterministic optimization I) $X5=200$, and II) $X5=270$

V. CONCLUSION

The software KEDRO developed for design of numerical and physical experiments, creating metamodels on basis of parametric and nonparametric approximations and multiobjective robust optimization can be used for practical optimization tasks with a small number (<12) of optimization variables. The test problem of two bar truss confirmed that it is possible to obtain a different solution considering structure optimization problem as non-deterministic. The uncertainties in pallet supports considerably affect the pallet rib shapes. The pallet manufacturing technology could be the main cause of uncertainties in design, e.g., improper dimensions and material properties due to characteristics of compression molding. In this case additional uncertainties must be considered during robust optimization.

REFERENCES

- [1] T. Sokół, and G. I. N. Rozvany. On the adaptive ground structure approach for multi-load truss topology optimization. Proc.10th World Congress on Structural and Multidisciplinary Optimization. May 19 -24, 2013, Orlando, Florida, USA, 10 p. (CD-ROM). Available: <http://www2.mae.ufl.edu/mdo/Papers/5428.pdf>
- [2] M. P. Bendsøe and N. Kikuchi, Generating optimal topologies in structural design using a homogenization method, *Comput. Methods Appl. Mech. Engrg.* 71 (2) (1988) 197-224.
- [3] M. P. Bendsøe and O. Sigmund, Material interpolation schemes in topology optimization, *Applied Mechanics*, vol. 69, pp. 635-654, 1999.
- [4] J. Haslinger, and R. A. E. Makinen, *Introduction to Shape Optimization: Theory, Approximation, and Computation*, SIAM, 2003, 273 p.
- [5] J. S. Arora, *Optimization of Structural and Mechanical Systems*, World Scientific, 2007, 595 p.
- [6] G. N. Vanderplaats, *Multidiscipline Design Optimization*, VR&D, 2007, 477 p.
- [7] R. T. Haftka, and Z. Gurdal, *Elements of Structural Optimization*, 3rd ed, Springer, 1992, 481 p.
- [8] A. Ben-Tal, L. E. Ghaoui, A. Nemirovski, *Robust Optimization*, Princeton University Press, 2009, 544 p.
- [9] A. E. Hami, and R. Bouchaib, *Uncertainty and Optimization in Structural Mechanics*, John Wiley & Sons, 2013, 144 p.

- [10] X. Du, and W. Chen, Towards a better understanding of modeling feasibility robustness in engineering design, *ASME J. Mech. Des.* 122, pp. 385-394.
- [11] A. Saxena, and B. Sahay, *Computer Aided Engineering Design*, Springer, 2005, 394 p.
- [12] T.H. Lee, and J.J. Jung, Metamodel-based Shape Optimization of Connecting Rod Considering Fatigue Life, *Key Engineering Materials*, VOL 306/308; 2006, pp. 211-216. Available: <http://citeseerx.ist.psu.edu/viewdoc/download?doi=10.1.1.111.4200&rep=rep1&type=pdf>
- [13] T. W. Simpson., A. J. Booker, D. Ghosh, A. A. Giunta, N. P. Koch, and R. Yang, *Approximation Methods in Multidisciplinary Analysis and Optimization: A Panel Discussion. Structural and Multidisciplinary Optimization*, vol. 27, 2004, pp. 320- 313.
- [14] D. C. Montgomery, *Design and Analysis of Experiments*, 8th ed, Wiley, 2012, 752 p.
- [15] S. Koziel, D. E. Ciaurri, and L. Leifsson, *Surrogate-Based Methods*, Chapter 3 in "Computational Optimization, Methods and Algorithms", Springer, 2011, pp. 33 -59.
- [16] C. E. Rasmussen, and Christopher K. I. Williams, *Gaussian Processes for Machine Learning (Adaptive Computation and Machine Learning)*, The MIT Press, 2005, 248 p.
- [17] J. Sacks, J.W. Welch, J. T. Mitchell, and H. P. Wynn, Design and analysis of computer experiments, *Statistical Science*, 4(4), Nov. 1989, pp. 409 -423.
- [18] J. Janusevskis, and R. Le Riche, Simultaneous kriging-based estimation and optimization of mean response, *Journal of Global Optimization*, vol. 55, issue 2, Springer, 2013, pp. 313-336. Available: <http://link.springer.com/article/10.1007%2Fs10898-011-9836-5>
- [19] D.S . Aponte, R. Le Riche, G. Pujol, and X. Bay, An Empirical Study of the Use of Confidence Levels in RBDO with Monte-Carlo Simulations, Chapter 9. in the book *Multidisciplinary Design Optimization in Computational Mechanics*, Edited by P. Breitkopf , R.F. Coelho, Wiley-ISTE, 2010.
- [20] A.R. Parkinson, R. Balling, and J.D. Hedengren, *Optimization Methods for Engineering Design*, Brigham Young University, 2013.
- [21] D. V. Rosato, D. V. Rosato, and J. Murphy, *Reinforced plastics handbook*, Elsevier, 2004, 586 p.
- [22] B. Davis, and P. Gramann, T. Osswald, and A. Rios, *Compression Molding*, Hanser Publication, 2003, 196 p.
- [23] A. Janusevskis, J. Auzins, A. Melnikovs, A. Gerina-Ancane, *Shape Optimization of Mechanical Components of Measurement Systems*, OAB Advanced Topics in Measurements, InTech, 2012, pp. 243-262. Available: <http://www.intechopen.com/books/advanced-topics-in-measurements/shape-optimization-of-mechanical-components-for-measurement-systems>
- [24] S. W. Tsai, and E. M. Wu, "A general theory of strength for anisotropic materials". *Journal of Composite Materials*. vol. 5, 1971, pp. 58-80.